

Advances in ALON optical component fabrication

J.E. DeGroot^{*}, N.B. Smith, J.J. Oliver, B.S. Piatt, M.P. Mandina, and R. Plympton
Optimax Systems Inc., 6367 Dean Parkway, Ontario NY 14519

L.M. Goldman and S.A. Sastri
Surmet Corporation, 31B Street, Burlington MA

Aluminum oxynitride, commonly referred to as ALONTM, is a transparent polycrystalline ceramic. ALON's transparency spans from the UV to the IR and it has excellent ballistic characteristics making it desirable for many military (IR domes and conformal windows) applications. ALON is formed into near net shape by conventional powder pressing techniques, but an optical finishing step is required to produce surfaces suitable for optical applications. In our work, we greatly reduced the overall ALON fabrication time by improving the rate and quality of the conventional grinding steps.

1.0 Introduction

Aluminum Oxynitride (ALONTM) is a hard cubic polycrystalline optical ceramic that is transparent from the ultraviolet (UV) to the mid-wave infrared (MWIR) region. ALON has similar mechanical properties to sapphire, with a Knoop hardness value four times harder than fused silica. ALON's optical and mechanical properties make it an excellent candidate for IR windows, domes, lenses and transparent armor.^{1,2}

Very little work in the open literature speaks to the conventional fabrication (grinding and polishing) of ALON. Two of the literature sources that do exist have shown that conventional fabrication of ALON has proven to be much more difficult compared to common optical glasses due to both its high hardness and polycrystalline grain structure.^{1,3} Initial results indicated that the loose abrasive lapping removal rates for ALON with 20um loose abrasive were non-linear with time (constant pressure and velocity). This effect was only magnified when polishing complex geometries such as domes and conformal windows. The obvious remedy would be to increase pressure and/or velocity⁴, unfortunately when working with complex geometries a fine balance exists between high removal rates and maintaining surface figure. In these situations, a need arises to find alternative ways to increase removal rates without adjusting the mechanical stroke (pressure and velocity) required to maintain surface figure.

This paper contains results from two separate experiments. The first section discusses how we systematically alter the surface tension of the carrier fluid for the loose abrasive lapping materials. The second section compares the sub-surface damage (SSD) of conventionally ground ALON to CNC generated and bound abrasive ground ALON. The SSD was measured using the MRF spot technique⁵ of the ground surfaces.

^{*} Contact Author: Phone: 585-265-1020 ext. 276, Email: jdegroote@optimaxsi.com

2.0 Experiment

2.1 – Carrier fluid surface tension experiment

One-inch diameter ALON™ plano-plano witness samples were ground with 40µm loose abrasive in an aqueous carrier fluid. The grinding experiments were all performed with a Strausbaugh 6Y-1 with a plano cast iron grinding lap. The over arm and spindle speeds were kept constant at 40 and 50 respectively. The weight (including the over arm) was also held constant at 6.5lbs. Four one-inch diameter ALON pieces were blocked using green blocking pitch on a 100mm cast iron plate that had a weight of 0.8lbs. The total weight for the system was 7.3lbs. Systematic additions of chemical C were made to the aqueous carrier fluid to alter the surface tension⁶ and the resulting removal rates and surface roughness values were recorded.

Removal rates were measured by recording height change in the ALON to the nearest 0.1µm. Four sites were averaged for each data point. Surface roughness was measured on the New View 200⁷. Data was recorded after 5-minute intervals.

2.2 – Sub-surface damage experiment

The HP-grade ALON material was supplied as a plate that was core drilled to produce twelve disks numbered 1 – 12. Side 1 was subjected to the conditions outlined in Table 1, which resulted in two disks having the surface texture of each grinding condition. [Note: The grinding conditions were chosen in order to get a comparison of SSD induced by the three different removal mechanisms, not necessarily based on the best possible outcome.]

Part #	Grinding method	Median abrasive size [µm]	Platform	Feed rate [mm/min]	Speeds		Load lbs.
					Bottom rpm	Top rpm	
1	Rough tool generate	62-74	SX-150	1	40	2500	-
2	Rough tool generate	62-74	SX-150	1	40	2500	-
3	Medium tool generate	10-20	SX-150	1	40	2500	-
4	Medium tool generate	10-20	SX-150	1	40	2500	-
5	Rough loose abrasive	40	Strausbaugh 6Y-1	-	50	40	7.3
6	Rough loose abrasive	40	Strausbaugh 6Y-1	-	50	40	7.3
7	Medium loose abrasive	20	Strausbaugh 6Y-1	-	50	40	7.3
8	Medium loose abrasive	20	Strausbaugh 6Y-1	-	50	40	7.3
9	Rough bound abrasive	30-40	Strausbaugh 6Y-1	-	50	40	7.3
10	Rough bound abrasive	30-40	Strausbaugh 6Y-1	-	50	40	7.3
11	Medium bound abrasive	10-20	Strausbaugh 6Y-1	-	50	40	7.3
12	Medium bound abrasive	10-20	Strausbaugh 6Y-1	-	50	40	7.3

Table 1 – SSD experimental grinding conditions

Removal rates were measured by recording height change in the ALON to the nearest 0.1µm. Three sites were averaged for each data point. Surface roughness was measured on the New View 200 for both the ground surface and inside the MRF spots.

Parts 1, 3, 5, 7, 9 and 11 were all subjected to etching at Surmet Corporation using their proprietary etching protocol. The etching step was done to confirm whether or not etching is required to open up the cracks in the surface to obtain an accurate SSD measurement.⁸ Etching removed ~1µm of material from the samples.

Nanodiamond MR fluid was loaded into the Q22-XE platform with the 50mm wheel in order to make the spots for SSD measurements. The viscosity was held constant at 45-46cP, the pump speed was 84rpm, the wheel speed was 850rpm, the ribbon height was 1.5mm and the spot depth was 0.5mm. The spotting times were 0.5, 1, 2, 3, 5, 7, 9 and 11 minutes. The depths of the spots were measured using a stylus profilometer.

3.0 Results

3.1 - Carrier fluid surface tension results

The experimental data collected from ALON™ ground with 20μm loose abrasive in an aqueous carrier fluid is shown in Figure 1. The decreasing removal rate with depth is obvious. Figure 1 also contains two data points collected from an ALON concave spherical grinding experiment with 20μm loose abrasive in the same aqueous carrier fluid, the pink square represents the removal rate (0.07μm/min) after 14μm was removed in the center and the green triangle represents the removal rate (0.02μm/min) after 3μm was removed from the edge. As one would assume when using a cap grinder the removal rate was higher in the center than the edge. The plano removal rates will always be higher compared to removal rates when grinding a spherical surface, but this one concave spherical surface was ground in order for us to make relative comparisons. Flat surfaces were used for all measurements from this point forward because the samples are easier to acquire, and it is straightforward to measure height variations and surface roughness values.

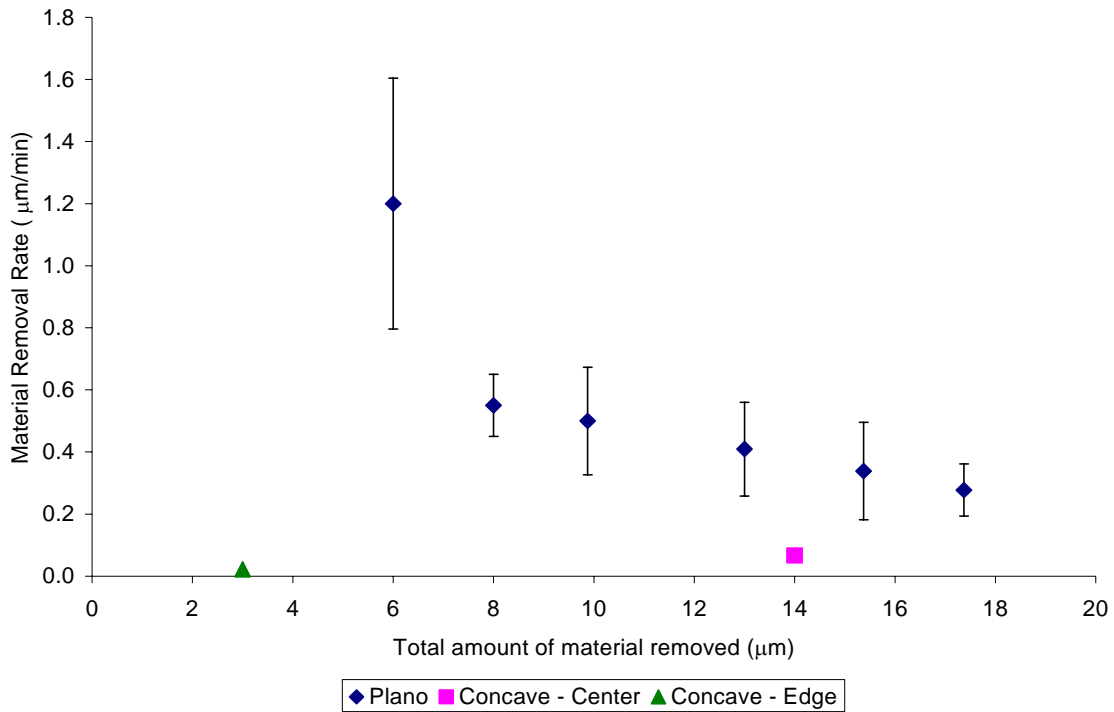


Figure 1 – Material removal rate versus total amount of material (ALON) removed using 20μm loose abrasive in an aqueous carrier fluid.

In Figure 2, the material removal rate is plotted versus total amount of material removed again, but also included in the plot is the initial areal peak-to-valley (PV) surface roughness of the ALON surface. [For example, each of the red circles represents the PV surface roughness of the ALON before the material removal rate data was taken.] The material removal rate appears to have a very high correlation to the PV surface roughness of the surface based on the data in Figure 3. Figure 3 is a plot confirming this high correlation. The confidence level for the linear fit is greater than 99%.

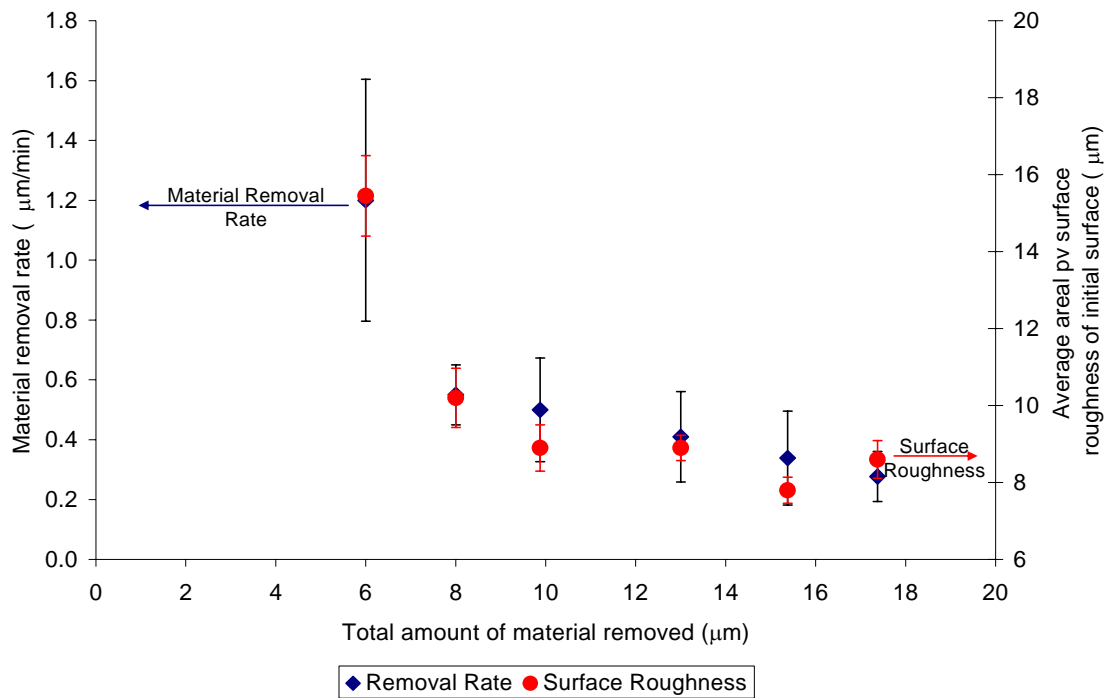


Figure 2 – Comparison of the material removal rate and the initial PV surface roughness.

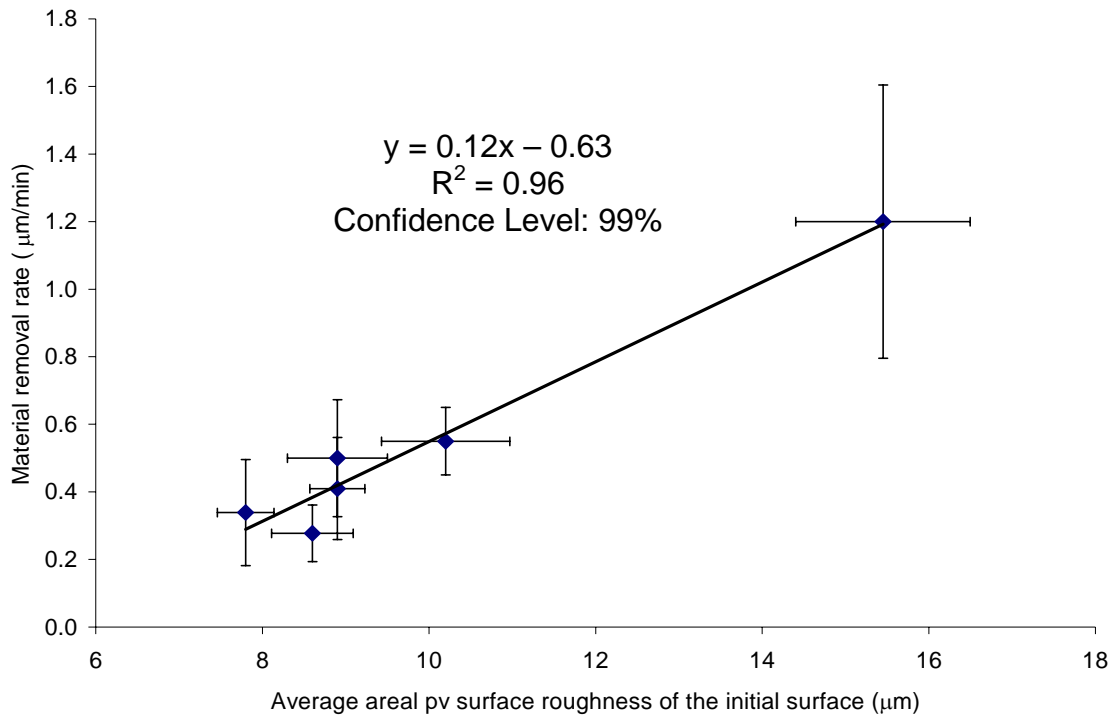


Figure 3 – Material removal rate versus PV surface roughness of the initial surface.

Based on the high correlation shown in Figure 3, the reason that the removal rate decreases significantly as more material is removed is due to how well the loose abrasive particles can fit between the cracks on the surface and remove material. The goal of this work was to increase material removal rate during the 20µm loose abrasive grind, to do this we altered the chemistry of the carrier fluid by using various amounts of chemical C (0 – 100%). The intent of chemical C was to lower the surface tension and allow for a better wetting of the ALON™ surface.

The various concentrations (weight percent) of chemical C in water are listed in Table 2 along with the corresponding surface tension values. The error for all surface tension measurements is +/- 0.5 dynes/cm, the error for the pH measurements is +/- 0.1.

Fluid	Surface tension (dynes/cm)	pH
Aqueous carrier	80	-
5wt% CC	78	6.7
10wt% CC	76	7.0
20wt% CC	73	7.2
40wt% CC	66	7.4
100% CC	56	7.9

Table 2 – Surface tension and pH measurements for various concentrations of chemical C (CC).

The major problem encountered when grinding ALON with the 20µm loose abrasive in the aqueous carrier fluid was removing material after removing 10-15µm of

material. At these depths material removal virtually stopped and whether it was figure error, center or edge thickness specifications or subsurface damage that needed the extra material removed, the material removal rate needed to be increased for economic reasons. Figures 4 and 5 plot the ALON™ material removal rate versus surface tension after 10μm and 15μm of material have been removed respectively.

The experimental results in Figures 4 and 5 indicate that there is an optimum value of surface tension for the carrier fluid when grinding ALON with 20μm loose abrasive. This optimum value occurs at 76 dynes/cm with a 10wt% chemical C concentration. The hypothesis for why this occurs is that the decreased surface tension from water increases surface wetting which allows the abrasive particles and carrier fluid to penetrate deeper into the cracks in the ALON increasing removal efficiency. Unfortunately, there is a point of diminishing returns where decreased surface tension stops increasing removal rates.

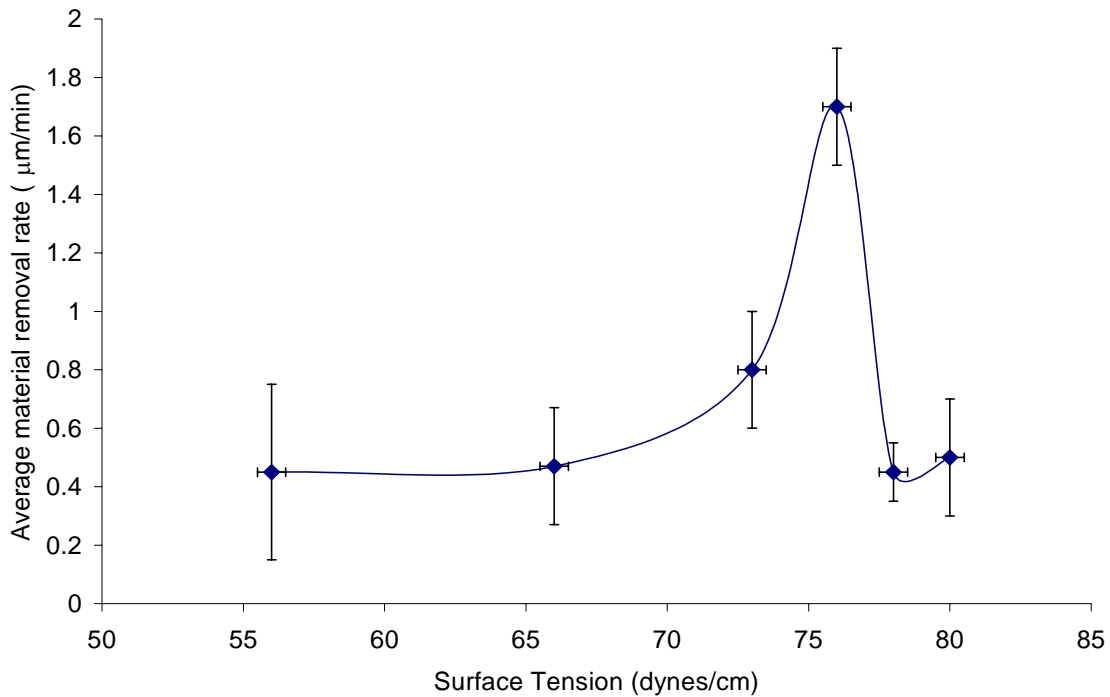


Figure 4 – Average ALON material removal rate versus surface tension of the carrier fluid. Results after 10μm of ALON had been removed with 20μm loose abrasive.

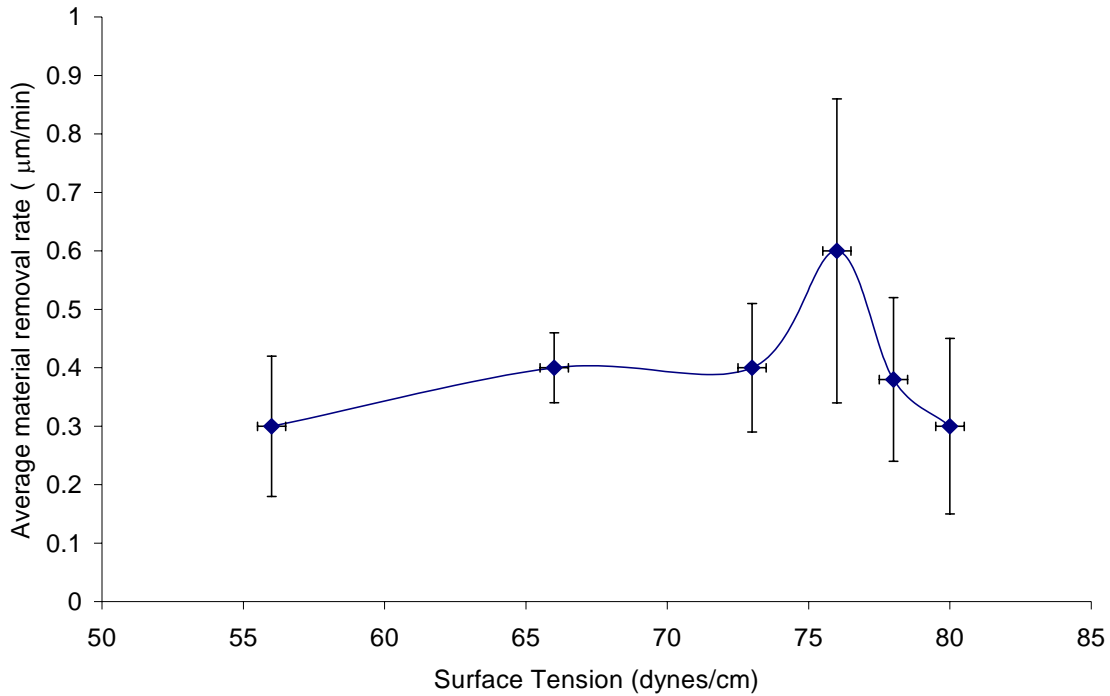


Figure 5 – Average ALON material removal rate versus surface tension of the carrier fluid. Results after 15µm of ALON had been removed with 20µm loose abrasive.

For the remainder of this paper we will focus on the 10% chemical C carrier in comparison to the aqueous carrier. The 10% chemical C carrier fluid with 20µm loose abrasive data is plotted with the aqueous carrier fluid data in Figure 6. This plot was previously shown as Figure 1. From this data, we observe that the removal rates are consistently ~2x higher for the 10% chemical C carrier fluid compared to aqueous carrier fluid. The higher removal rates caused the data points for the 10% chemical C to occur at deeper into the ALON™. Both experiments were run for a total of 40 minutes and the 10% chemical C carrier fluid removed 9µm more material than the aqueous carrier fluid.

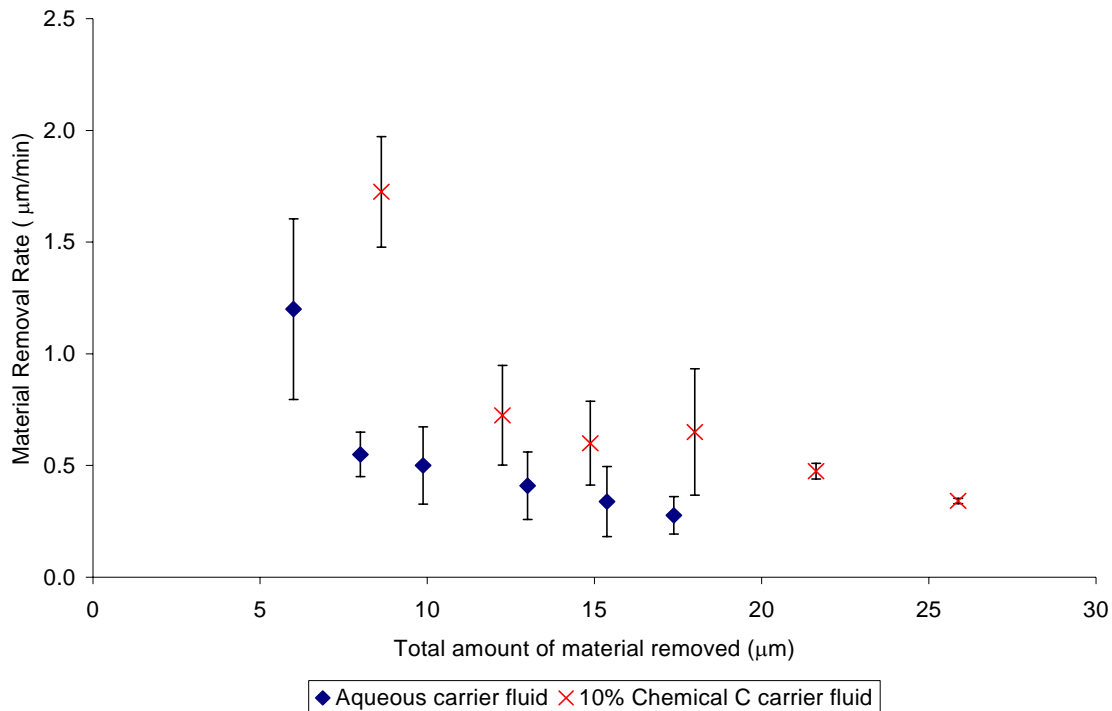


Figure 6 – Material removal rate versus total amount of material removed for 20µm loose abrasive.

In Figure 7, the same data shown in Figure 2 is plotted again (on the same scale as Figure 2) with the corresponding 10% chemical C data. Figure 7 plots the material removal rate versus total amount of material removed along with the PV surface roughness for the initial surface for each step. The initial PV surface roughness after the 40µm loose abrasive grind was the same for both experiments, although the removal rate for the 10% chemical C carrier fluid was higher than the aqueous carrier fluid. One of the most interesting observations from Figure 7 is the fact that the PV surface roughness for the 10% chemical C carrier fluid was slightly lower than aqueous carrier fluid surface roughness values. The 10% chemical C data is plotted again in Figure 8 on a slightly different scale so that the left most data points are aligned. Unlike the aqueous carrier fluid data, there is not a very strong correlation between PV surface roughness and material removal rate. The PV surface roughness immediately reduces to slightly lower than 7-8µm and there is no change as more material is removed. This data shows us that with the use of a carrier fluid with lower surface tension that we can “push out” our dead end in ALON™ material removal rates.

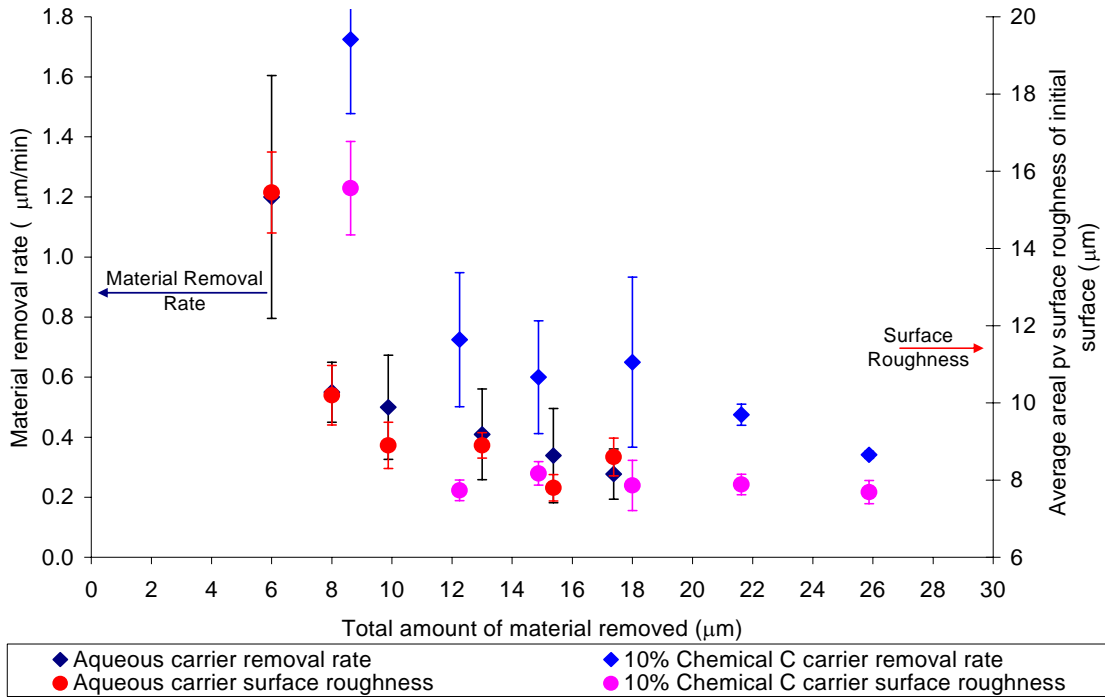


Figure 7 – Material removal rate and average areal PV surface roughness of the initial surface versus the total amount of material removed

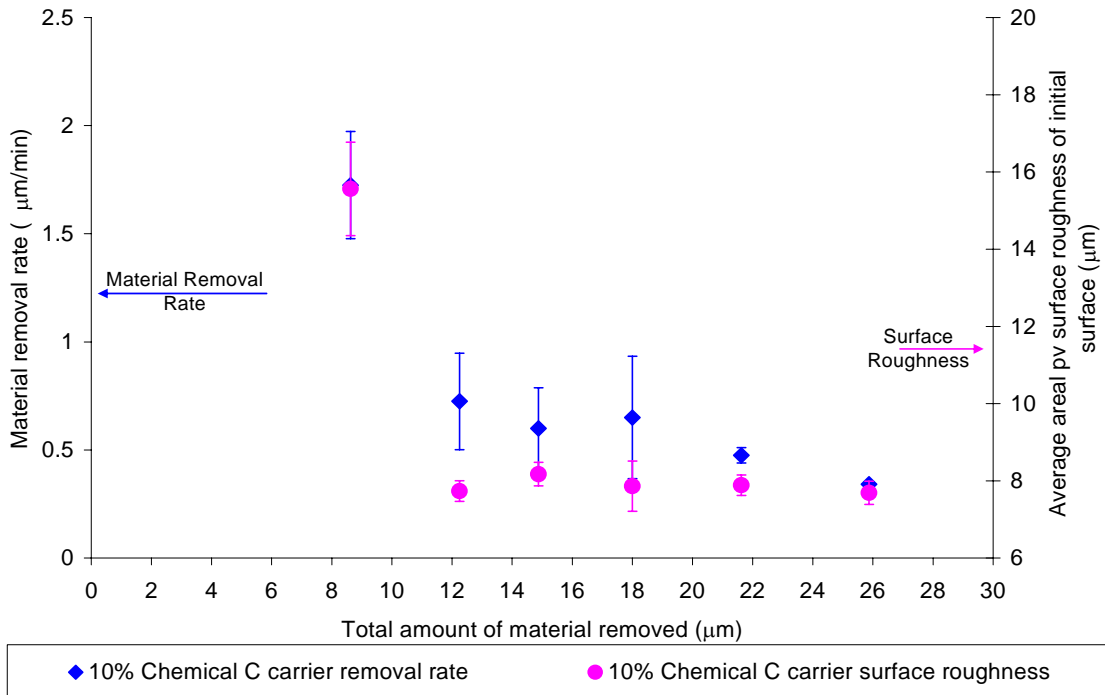


Figure 8 – Material removal rate and average areal PV surface roughness of the initial surface versus the total amount of material removed

For comparison, the root-mean-square (rms) surface roughness values are plotted versus the total amount of material removed in Figure 9 for both the 10% chemical C and aqueous carrier fluids. The data is included with the material removal rate data similar to Figures 7 and 8. Other than the first removal point there does not appear to be a correlation between rms surface roughness of the surface prior to grinding and the material removal rate.

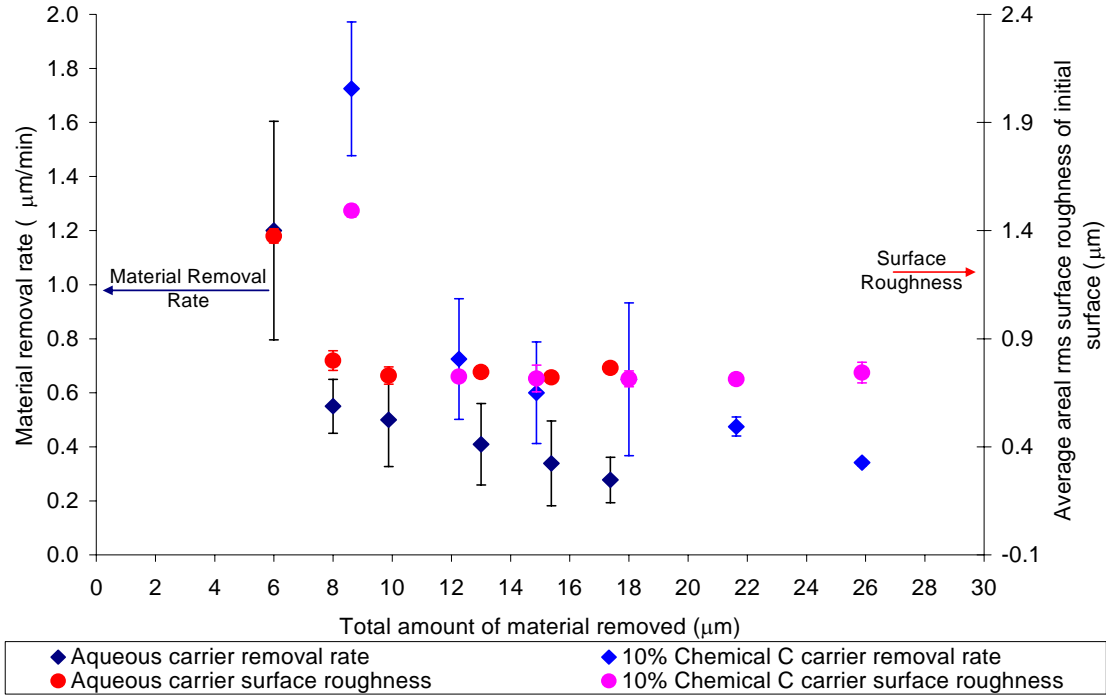


Figure 9 – Material removal rate and average areal rms surface roughness of the initial surface versus the total amount of material removed.

3.2 – Sub-surface damage results

The SSD present after CNC grinding has been determined to be less than the PV surface roughness measured with a white light interferometer.⁵ We extended this work to examine loose abrasive conventionally ground surfaces and bound abrasive ground surfaces. The experimental outline was given in Table 1 in Section 2.0.

Figure 10 shows the SSD experimental results for the rough generated ALON™ surfaces that were measured of the as-ground and etched surfaces. The amount of SSD is determined by finding the intersection of the two best fit slopes (see Ref: 5). For the medium tool generated surface the SSD was 8.1µm for the etched surface and 9.2µm for the unetched surface. Through comparison of the etched to unetched SSD measurements, (see Table 3) we observe that the etched surface had lower SSD values compared to the as-ground surface. We conclude from this that the etching step is not required to open up the radial cracks induced during grinding in order to determine the amount of SSD.

Comparisons between grinding mechanisms will be made using the SSD measured from the as-ground surface.

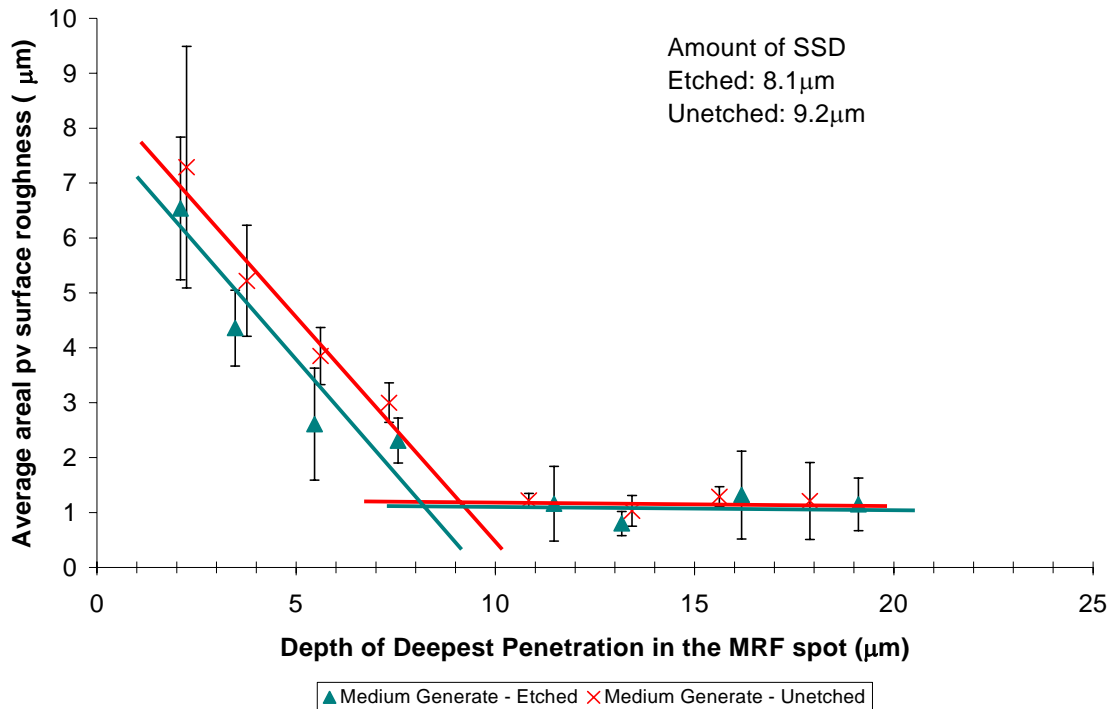


Figure 10 – Average PV surface roughness versus MRF spot depth.

Part #	Surface treatment		SSD [μm]
1	Etch	Rough Generate	17.7
2	As-ground	Rough Generate	21.9
3	Etch	Medium Generate	8.1
4	As-ground	Medium Generate	9.2
5	Etch	Rough Loose	8.8
6	As-ground	Rough Loose	9.5
7	Etch	Medium Loose	5.9
8	As-ground	Medium Loose	7.5
9	Etch	Rough Bound	14.9
10	As-ground	Rough Bound	15.3
11	Etch	Medium Bound	6.7
12	As-ground	Medium Bound	11.2

Table 3 – SSD values for each surface treatment. Average error for each measurement +/- 10% (~1 μm).

The SSD data for the as-ground surfaces in Table 3 is plotted versus the average areal PV surface roughness measured on the as-ground surface with a white light interferometer in Figure 11. The line drawn indicates a one-to-one relationship between PV surface roughness and SSD. All of the data points are above this line, which indicates

that the SSD of ALON™ is always less than the PV surface roughness of the ground surface.

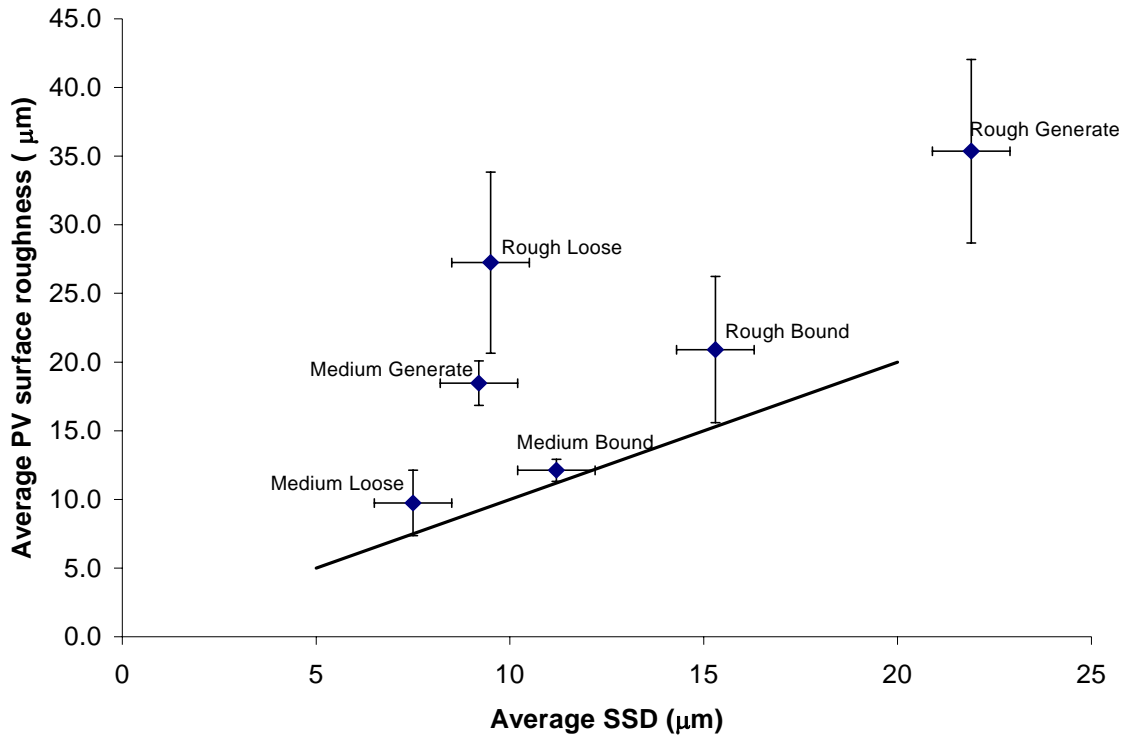


Figure 11 – Average PV surface roughness versus average SSD for the six different surface treatments. The labels next to each data point indicate the grinding technique.

In addition to estimating the SSD based on PV surface roughness, the SSD can also be correlated to the grinding removal mechanism and abrasive particle size. Figure 12 shows a plot of the median particle size versus the measured average SSD for all six grinding methods. This plot indicates that the loose abrasive (three-body abrasion) method produce the lowest amount of SSD as a function of median particle size, but they also have the steepest slope indicating that decreasing the loose abrasive size will not offer too much advantage in terms of shorter polishing times. [Polishing must remove the amount of material equal to the SSD for each grinding method.] The remaining data points are all two-body abrasion methods and higher SSD values. This contradicts what Lambropoulos⁹ found for brittle materials (glass) where he found that deterministic microgrinding consistently gave surfaces of lower SSD for the same abrasive size as conventional grinding.

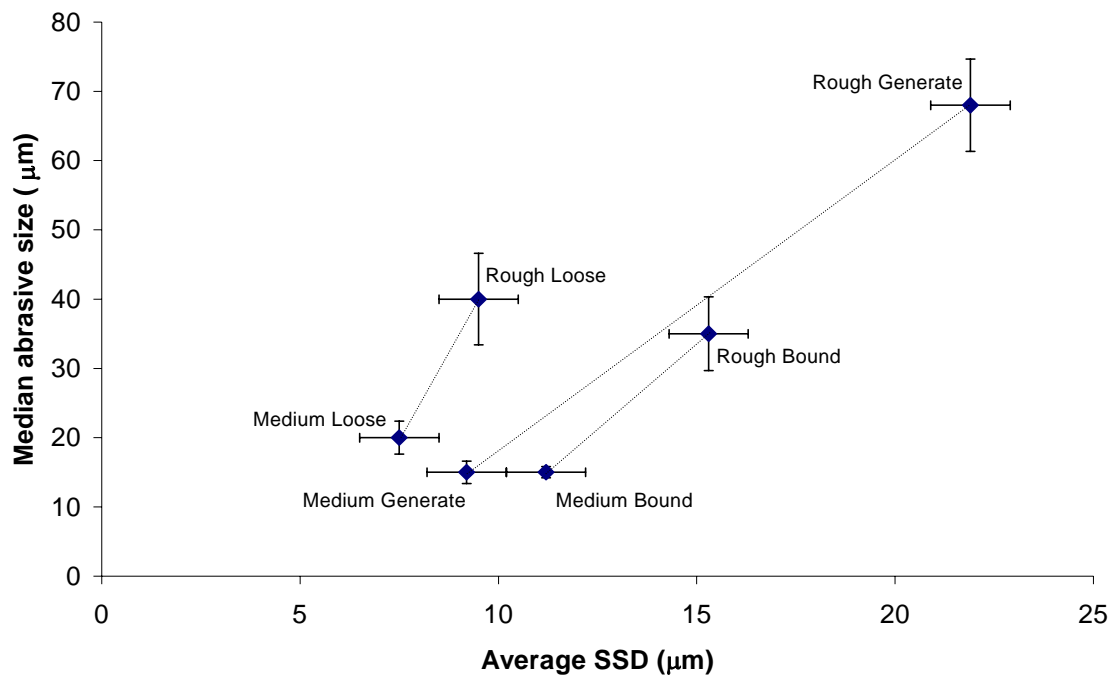


Figure 12 – Median abrasive size versus measured average SSD for the six different surface treatments. The surface treatments are indicated next to each data point. Lines have been drawn to guide the eye.

4.0 Conclusion

In this work, we systematically altered the surface tension of the carrier fluid for the loose abrasive lapping materials. We were able to increase ALON™ grinding material removal rates by a factor of two by only adjusting the surface tension of the carrier fluid, holding all other variables constant (pressure, speed, temperature, etc.). In addition, we confirmed what was determined in previous work that the SSD is less than the average areal PV surface roughness value measured with a white light interferometer and etching is not required to accentuate radial cracks formed during grinding. Loose abrasive grinding produced the lowest SSD values for similar abrasive size compared to CNC generating tools and bound abrasives. These initial results appear to be contradictory to what was previously found for brittle materials. Additional work will determine to what extent this relationship holds true.

References

1. J. M. Wahl, T. M. Hartnett, L. M. Goldman, R. Twedt, and C. Warner, "Recent Advances in ALON™ Optical Ceramic," in *Window and Dome Technologies and Materials IX*, R. W. Tustison, ed. (SPIE, Orlando, FL, 2005), pp. 71-82.
2. "Surmet Corporation, 33 B Street, Burlington MA, www.surmet.com."
3. L. L. Gregg, A. E. Marino, and S. D. Jacobs, "Grain decoration in aluminum oxynitride (ALON) from polishing on bound abrasive laps," in *Optical Manufacturing and Testing V*, H. P. Stahl, ed. (SPIE, San Diego, CA, 2003).
4. F. W. Preston, "The theory and design of plate glass polishing machines," *Journal of the Society of Glass Technology* **11**, 214 - 256 (1927).
5. S. N. Shafrir, J. C. Lambropoulos, and S. D. Jacobs, "Subsurface damage and microstructure development in precision microground hard ceramics using magnetorheological finishing spots," *Applied Optics* **46**, 22, 5500-5515 (2007).
6. "Fisher Scientific Surface Tensiomat (Model 21, Catalog# 14-814)."
7. "Zygo NewView 200, 20x Mirau objective, 40μm scan length, no phase averaging, unfiltered, remove spikes: off."
8. Y. Zhou, P. D. Funkenbusch, D. J. Quesnel, and A. Lindquist, "Effect of etching and imaging mode on the measurement of subsurface damage in microground optical glasses," *Journal of American Ceramic Society* **77**, 12, 3277-3280 (1994).
9. J. C. Lambropoulos, "What mechanics and materials science can do for the modern optical workshop," in *Fall 1999 Workshop*, (APOMA, Rochester, NY, 1999).